SPATIOTEMPORAL CHAOS OF PANEL OSCILLATION FORCED BY TURBULENT BOUNDARY LAYER AND SOUND

L. Maestrello*
NASA Langley Research Center
Hampton, VA. 23681

Abstract

Conclusive experimental evidence is presented for spatiotemporal chaos response of two adjacent aircraft panels that are forced by a turbulent boundary layer and pure tone sound. The experiments are a simulation of boundary-layer and fan noise loads on a fuselage sidewall with Reynolds number per meter of 2.85×10^5. The response of the panels is linear when forced by the turbulent boundary-layer flow, and nonlinear from periodic to spatiotemporal chaotic when forced by the boundary layer with superimposed pure tone sound. The periodic response with two tori of two commensurable frequencies changes with increases in pure tone sound level. The first change is to period-doubling bifurcations that then transition to spatiotemporal chaos, which alternates with quasi-periodic response as the wave loses the spatial homogeneity while localized wave holes or chaotic patches form. Periodic response, low order spatiotemporal chaos, and then broadband spatiotemporal chaos with finite N-wave response is investigated. The objective is to demonstrate the existence of strong nonlinearity on the structure response, which would require future investigations of flow, structure, and high intensity sound interactions.

1. Background

Most studies of nonlinear deterministic and stochastic dynamic systems examine externally excited systems. A typical example of an externally excited system is an aircraft fuselage structure interacting with the turbulent boundary layer and jet engine noise. Periodic, aperiodic, and chaotic responses can occur along the sidewall of the fuselage structure during acceleration from take-off to cruise altitude, as well as at cruise altitude. One type of load is buzz-saw noise in high-bypass ratio turbofan engines. The present experiment is designed to simulate such loads, as well as structural nonlinear responses that result from turbulent boundary layer flow and high intensity sound interaction. Such experiments must be conducted in a wind tunnel with an anechoic test section to prevent standing wave formation between the test panel surface and the opposite sidewall of the tunnel.

In previous experiments, panels with periodic nonlinear responses to sound and flows of constant or accelerated speeds and active control were considered [1,2]. This study simulates classes of abnormal processes of flow and sound loads, unsteady loads of the boundary-layer pressure fluctuations coupled with the panel responses, and sound radiation by the panel. Presently, nonlinear behaviors that result from increasing levels of pure tone sound so that the responses change from periodic to broadband spatiotemporal chaos with weak shocks or N-waves are investigated. Although the disorder or spatiotemporal chaos is often related to a large extended structure, the experiments indicate that spatiotemporal chaos exists in localized responses within a panel. Much has been observed about temporal chaos, while little is known about spatiotemporal chaos [3,4]. New tools to interpret the observed dynamics will be described. In the past, chaotic signals were not exploited as physical behavior, but were hidden in the broad view given by the stochastic processes. We are now able to distinguish between periodic, quasi-periodic, and nonperiodic responses. By varying the input acoustic load superimposed on the turbulent boundary-layer flow, instability leading to periodic responses can be observed. With increased loads, the responses convert from periodic to quasi-periodic and then to chaotic, analogue to that reported in references 5 and 6. This characteristic route to chaos was suggested by Grebogi et al, Newhouse et al, and Dowell, [7,8,9]. In our experiments the loads and responses are typical of certain aircraft maneuvers and simulate the Reynolds number of the turbulent boundary layer, the acoustic pressure signature of a turbofan engine, and the panel size. Results of the input load, panel response, and sound transmission are discussed. Specifically we focus

*Senior Research Scientist, Associate Fellow

on the following: turbulent boundary-layer response with and without acoustic forcing; panel with periodic, low, and high order spatiotemporal chaotic responses; and the acoustic pressure transmitted to the cabin side by the panel oscillations.

The paper is divided into four sections. Section 2 describes the experimental setup. Section 3 describes the turbulent boundary layer and then the turbulent boundary layer with added pure tone sound is described in section 3.1. In section 3.2, the panel responses changing from periodic to spatiotemporal chaos responses are described. In section 4, the transmitted pressure is discussed. In section 5, the results and some conclusions are summarized.

2. Experimental Apparatus and Instrumentation

The apparatus, an open circuit wind tunnel, has been described at length in studies of constant and accelerated boundary-layer flow experiments [1,2]. The present experiments are conducted with two aluminum aircraft fuselage panels that are joined by a stringer mounted on a rigid baffler. (See fig.1.) Two panels are necessary to allow wave transmission from one to another when forced by convecting loads. The panel sizes are 0.65 m by 0.20 m by 0.001 m and the stringer cross section is 0.0128 m by 0.0128 m. The test section is anechoically designed to study boundary layer and sound interaction problems. The Reynolds number per meter of the turbulent boundary layer is $R_e/m = 2.85 \times 10^5$, free stream velocity is $U_e = 46$ m/s, and boundary layer thickness is 0.060 m. The acoustic sources are created by four 120 watt phase-amplitude matched speakers that are mounted on a diffuser within the anechoic sidewall and facing the downstream panel. (See fig. 1.) The forcing frequency of the speakers is 960 Hz at sound power level of 138 dB, which is needed to obtain spatiotemporal chaos response at the panel surface. The sound power level of 130 dB is used to produce low order spatiotemporal chaos at 505 Hz. In earlier experiments, the highest power level of acoustic excitation was a factor of two to four lower than the 130 dB level used here. The wall pressure fluctuation and the radiated pressure are measured by miniature pressure transducers, the velocity is measured by hot wire anemometer, and the vibration response is measured by miniature accelerometers. All measurements are made from direct current response.

3. Transition from Periodic to Chaotic Responses

In this section, the tools used to analyze the dynamics of the panels responses and to characterize the oscillations forced by turbulent boundary layer or by turbulent boundary layer with pure tone sound are explained. The time history of the wall pressure fluctuation panel acceleration are measured. From the time history, the power spectrum density, the phase portrayal, and the probability distribution, and the Liapunov exponent are evaluated [10,11,12]. For a nonstationary signal q(t,x), such as the pressure fluctuation p(t,x) or the panel acceleration g(t,x), the instantaneous power spectrum at instant T is defined by

$$P(f,T) = \left| \frac{1}{2\pi} \int_{T-I/2}^{T+I/2} \exp(i2\pi ft)\, q(t,x)\, dt \right|^2$$

where T is chosen so that the experimental run contains the interval (T - I/2, T + I/2) for a sufficiently large I. The Liaponov exponent of the panel acceleration is define by

$$\lambda(E,x) = \frac{1}{E} \ln \left\{ g(T,x) \Big/ \left[\int_0^E g^2(t,x)\, dt \right]^{1/2} \right\}$$

where E denotes the duration of the run. The following table illustrates the experimental stages used to analyze the wall pressure and panel responses.

Two classes of waves are present in the boundary layer and in the panel response: convecting waves and nonconvecting or kinematically generated waves. The waves are defined by a nonzero and a zero phase shift response, respectively and are also found in free shear layers [13–17]. The convecting waves are induced by turbulent eddies moving in the boundary layer that drive the panel oscillation, while nonconvection occurs across the boundary layer. The spacial scale in the boundary layer along the direction of flow is approximately equal to the boundary layer thickness. For the panel, the surface waves propagate over several thicknesses.

3.1 Turbulent Boundary Layer Without and With Pure Tone Sound

Upstream of the test section, the boundary-layer thickness is artificially increased by putting sandpaper on the tunnel sidewall. As a result, the Reynolds number based on the boundary-layer thickness increases and becomes consistent in scale with current aircraft fuselage boundary layer. The structural size of the panels is also typical of those used in aircraft fuselage sidewall panels. The mean velocity profiles of the turbulent boundary layer are measured downstream of the second panel for the turbulent boundary layer alone

Table 1. Panel Forcing and Response Enroute to Spatiotemporal Chaos

Force	Response (bifurcation state)
Turbulent boundary layer in absence of sound	Broadband linear, surface waves convecting with flow
Turbulent boundary layer with pure tone sound	Periodic with two or more commensurate frequencies superimposed on broadband
Turbulent boundary layer with increasing pure tone sound amplitude	Low frequency spatiotemporal chaos
Turbulent boundary layer with higher pure tone sound amplitude	Broadband spatiotemporal chaos with N-waves

and the turbulent boundary layer with the added pure tone sound at different amplitude levels. The results show that the turbulent boundary-layer thickness increases slowly as the amplitude level increases.

The real-time wall pressure is measured at the center of the stringer supporting the two panel, because the pressure transducer can not be mounted on the panel without altering the response of the panel. The measured real-time pressure p(t), the computed power spectral density P(f,T), phase plots $\dot{p}(t)$ versus p(t), and probability density Q(r,T) are shown in figure 2(a) for turbulent boundary layer without external sound. Figure 2(b) shows the same for boundary layer with pure tone sound at 960 Hz and 138dB sound power level. The real-time pressure p(t), shown for an interval of 0.5 sec in figures 2(a) and 2(b) near the instant T, is used for the evaluation of the instantaneous plots of spectrum, phase, and probability. Also note that the scales for the pressure fluctuations for figures 2(a) and 2(b) are in the ratios of 5 and 40.

Figure 2(a) shows a typical turbulent boundary-layer pressure fluctuation with broadband spectrum and convective phase portrait and nearly Gaussian distribution. Figure 2(b) shows the effect of added pure tone sound to the level of 138 dB on the change of the amplitude of pressure fluctuation and the appearance of the peaks corresponding to the pure tone sound. In the spectrum plot, the peaks of the pure tone sound are almost 30 dB higher with harmonics and subharmonics superimposed on the broadband spectrum. The amplitude of the broadband spectrum in figure 2(b) becomes nearly constant, while that shown in figure 2(a) is higher at the low frequency end. This difference in broadband spectrum shows that the distribution of energy in boundary layer is significantly altered by incident pure tone sound. The real-time pressure fluctuation shown in figure 2(b) consists mainly of N-waves of nearly constant amplitude , while the broadband fluctuation is not observable because of the larger scale needed for the N-waves. In the spectrum plots, the peaks of the pure tone and the second harmonics are nearly 30 dB above the broadband. In addition there are peaks of higher harmonics and subharmonics. In the phase portrait, the convective effect is overshadowed by the effect of the high power level sound at normal incidence. The probability plot is clearly non-Gaussian and has a much larger frequency range than that in figure 2(a).

3.2 Panel Response

The static pressure inside the wind tunnel is below the ambient pressure outside, which simulates aircraft panels in flight when the ambient pressure outside the fuselage is below the ambient pressure inside the cabin. Thus, the panels in the wind tunnel tend to deflect toward the moving stream. The mean static deflection is approximately the panel thickness or less. Because of the difficulty of mounting a pressure transducer on a moving surface without changing the inertial of the surface, the panel acceleration is measured instead. The accelerometers on the downstream panel B are placed along the center line at 1/4 and 3/4 panel length. (See fig.1.) Note that the panel acceleration is related to the load, that is, the wall pressure difference.

(a) Transition to Periodicity

The real time acceleration response g(t), measured on the center line at 3/4 panel length is shown in

figure 3(a) for a turbulent boundary layer without the incident pure tone sound and in figure 3(b) with added pure tone sound at 960 Hz and 130 dB level. The time history of the response g(t) in figure 3(a) shows a random modulate amplitude with nearly Gaussian probability distribution $\overline{Q}(r,T)$. The power spectral density G(f,T) and phase portrait $\dot{p}(t)$ versus p(t) show typical random broadband response. Thus the panel response shown in figure 3(a) is qualitatively similar to the wall pressure fluctuation without the incident sound in figure 2(a).

In the presence of sound, the pure tone level is set at 130 dB and 960 Hz so that the response of panel B is periodic, as shown in figure 3(b). In the spectrum plots, there are peaks of the pure tone frequency, harmonics, and subharmonics. The subharmonics were absent in the earlier experiments for which the pure tone frequency and power level were lower. The quasi-periodic response and phase locking of two frequencies f_1 and f_2 are evident. The forcing frequency f_1 is 960 Hz. The spectral density shows that the lowest subharmonic f_2 to be $f_1/5$. All peaks are linear combinations of f_1 and f_2. Thus the phase and probability plots show periodic responses commensurable to f_1 and f_2. This observation is relevant to several recent developments in nonlinear dynamics [13, 18–25].

(b) Transition to Chaos

With increasing pure tone sound level in the presence of the turbulent boundary layer, the panel oscillation exhibits nonperiodic responses. In real time, spacially incoherent behaviors are presented at two locations on the surface. In these locations, the responses are chaotic in the low and high frequencies ranges, which distinguishes the low dimensional from the broadband chaos. The wall pressure fluctuation load is known to decay exponentially with distance. Measurements indicated that panel response also decays with distance, but at a slower rate, which is evidence of spatial dispersion. Measurements between these two locations show that the localized response is weak. Because these two locations are far apart, their interaction is also weak. Thus, spatially localized chaotic responses are spatiotemporal.

First the low frequencies response of panel B with pure tone at f_2 = 505 Hz is discussed. This pure tone frequency is an attempt to trigger low order chaos response instead of broadband chaos response. Low order chaos in the region below the forcing frequency $f < f_1$ is characterized by a low number of degrees of freedom. The acceleration response at the surface of the panel at 1/4 and 3/4 panel length are different as shown in figures 4(a) and 4(b). The phase plots are nonperiodic and chaotic in character and vary with different dynamics at each location. This difference implies that more than a single chaotic domain is involved. Successive responses indicate that continuously moving domains are created and destroyed as time evolves. To substantiate a chaotic state we evaluate the Lyapunov exponent, which indicates values between 1.8 to 2.5. In the frequency domain, the spectra displays several peaks below the force frequency. The two spectra have different low frequency responses and levels. The probability indicates departure from periodicity as well as different distribution between locations. Additional differences are evident in the real-time plot shown in figure 4(a). Furthermore, figure 4(a) indicates randomness in amplitude, while figure 4(b) indicates a finite amplitude wave. From these results, we can conclude that the chaotic low frequency response is spatiotemporal.

At higher pure tone sound level and at a higher force frequency of 960 Hz, a nonuniform rise in the broadband spectrum at both locations is observed in figures 4(c) and 4(d). The formally periodic responses of the time and phase data records, partially shown in figure 3(b), become irregular and the entire record appears nonperiodic. The corresponding phase data plots appear completely chaotic and intermix with quasi-periodic oscillation diverging with time in figure 4(c). Again the chaotic state is substantiated by the Lyapunov exponent, which indicates values between 2.4 and 3.5 that are consistently positive and higher than lower order chaos responses. Temporal responses indicate the existence of complicated independent spatial pattern or multiple domains. The spectra, as well as the probability plots, have broadband chaotic spatiotemporal behaviors. Extended real-time response (not shown) indicates spontaneous random switches between quasi-periodic and chaotic behaviors at the two locations. The spontaneous switching seems to be the generalization of induced intermittence by the boundary-layer instability due to finite amplitude waves from the acoustic field. This alteration from spatiotemporal chaotic to quasi-periodic behavior corresponds to an involved sequence of bifurcations which terminate when a new divergency in the phase plots is created or lost. The power spectrum of the panel response is not so clear as the information obtained from phase plots. After a short period of time, the phase orbits split (fig. 4(c)) and never quite retrace themselves, which indicates

that the motion occurs at an incommensurate frequency. This occurrence is an indication of loss in stability. The spatiotemporal response indicates that new domains are created and destroyed, which maintains spacial incoherence. (See figs. 4(c) and (d)). From the data, we can establish that the combined turbulent boundary layer and pure tone sound are the sources that trigger spatiotemporal behaviors. In an earlier experiment when the panel was forced by high intensity sound alone, the response was temporal chaotic [23]. Additional experimental results by Gollup et al and Matsumoto et al. have indicated that chaotic instability depends on the characteristics of the external noise field, a consideration well established and consistent with present results [3,4,11].

Additional features of the wall pressure fluctuation and panel responses can be noted from the time plots (figs. 2(c) and 4(d)), which indicate that forcing and response are induced by finite amplitude N-waves responses. The presence of N-waves is attributed to the high level of the acoustic pure tone impinging on the turbulent boundary layer. For practical consideration, the pure tone level is comparable with the sound level of a turbofan engine. A video tape utilizing a real-time response illustrates additional features that are possibly not evident from the instantaneous data.

4. Wave Transmitted Through the Panels

The turbulent boundary layer induces panel vibration that in turn induces acoustic pressure in the ambient medium outside the tunnel, which simulates cabin noise. A pressure tranducer is placed 0.79 m from the downstream panel B at the center outside the flow field. To prevent acoustic interference, the exterior surface of panel A is covered with acoustic insulation material. Figure 5(a) shows the result, of only turbulent boundary-layer panel loads and figure 5(b) shows turbulent boundary layer and pure tone sound loads at the higher force amplitude. (See table 1.) The plots include the following: the real time p(t), power spectral density P(f,T), phase $\dot{p}(t)$ versus p(t), and probability density distribution $\bar{Q}(r,T)$. The pressure transmitted by the panel and forced by turbulent boundary layer alone is random broadband, similar to the wall pressure fluctuation and the vibration response with Gaussian type probability distribution. The transmitted pressure in the presence of high level pure tone sound is also broadband with a superimposed N-wave field that originated from the wall pressure load (fig. 2(b)) and was transmitted by the panel motion (fig. 4(d)). The power spectral density is chaotic. The transmitted probability distribution is non-Gaussian and the phase is nonperiodic. Like the panel response, the amplitude of the transmitted pressure changes with time over a wide range from spatiotemporal chaos to quasi-periodic. The acoustic pressure is nonsymmetrical with respect to the panel center similar to the panel response. Thus, nonlinear acoustic waves have practical applications to the simulation of cabin noises, in addition to theoretical interest.

5. Discussion and Conclusion

Spatiotemporal instability of periodic or chaotic panel responses forced by turbulent boundary layer and pure tone sound was investigated to study sequences of bifurcations as the pure tone sound level increases. From an initial state, the turbulent boundary-layer flow with superimposed pure tone sound makes the response of the panel go through a reproducible sequence of period-doubling in the first stage and, as the tone level increased, the response of the panel goes through breaking of the period-doubling and loss of partial coherence in the final stage. In particular, the following behaviors were observed as the sound level increased:

a) The wall pressure fluctuation and the turbulent boundary layer was altered by the pure tone sound. The pure tone and harmonics levels exceed the broadband level by 30 dB in sound power level. This was accompanied by a reduction of the lower frequencies broadband level (fig. 2). As a result the pure tone sound coupled with the turbulent boundary layer modified the boundary-layer thickness and the spatial correlation and the load on the structure.

b) The coupling between the acoustic load and the turbulent boundary-layer load on the panel induced first periodic response to the panel. The periodic response was composed of two coupled attracting regions whose trajectory made transition from one to the other through the commensurable subharmonic frequency f_1 coupled to the force frequency f_2. As a result, the power spectral density was a series of peaks at all integer combinations of two commensurable frequencies f_1 and f_2. Any other choice of reference frequency is related to these two frequencies. (See fig. 3.)

c) As the level of the pure tone increased, the panel response bifurcates from periodic to spatiotemporal chaos, and as such, the waves lost the special homogeneity responses and localized wave holes or chaotic patches formed randomly (fig. 4). One significant feature was that the response was not steady, but randomly altered from chaotic to quasi-periodic. Some behaviors are shown in the real-time video. The

continuous variation is an indication that the responses have nonstationary statistics since the non-periodic responses have no steady average. The dynamics may be similar to the observation made by Gollup and Benson in which phase locking convection alternates between quasi-periodic and periodic responses. The wave field behaved somewhat like the turbulent boundary-layer convecting pressure field; the localized acoustic load introduces changes in amplitude and in spatiotemporal distribution. The combined turbulent boundary-layer and acoustic load cause an increase in complexity so that the response field becomes transient and dispersive. In spite of recent results, the whole nonlinear-nonstationary problem in structural dynamics is still not satisfactorily understood.

Control of spatiotemporal chaos due to turbulent boundary layer and sound on a panel is more complicated that the periodic responses. Low order chaos (figs. 4(a) and (b)) contain fewer modes, and as such, control of the dynamics may be realizable.

Part of the response feature can best be understood when viewed in real time. Thus, segments of the experiments are recorded on video tapes. These tapes will be shown at the AIAA/CEAS Aeroacoustic Conference, May 12-14, 1997.

References

1. Maestrello, L., "Control of Panel Response to Turbulent Boundary Layer and Acoustic Excitation", *AIAA Journal*, Vol. 34, No. 2, 1966, pp. 259–264.

2. Maestrello, L., "Active Control of Panel Oscillation Induced by Accelerated Turbulent Boundary Layer and Sound", (accepted for publication in the *AIAA Journal*).

3. Gollub, J. B., and Benson, S. V., "Many Routes to Turbulent Convection". *Journal of Fluid Mechanics"*, Vol. 100, 1980, pp. 449–471.

4. Gollub, J. P., and Ramshanker, R., "Spatiotemporal Chaos in Interfacial Waves", New Perspectives in Turbulence, edited by L. Sirovich, Chapter 6, Springer-Verlag, pp. 165–194.

5. Screenivasan, K. R., "Transition and Turbulent in Fluid Flow and Low-Dimensional Chaos", *Frontier in Fluid Mechanics*, edited by S. H. Davis and J. M. Lumley, Springer-Verlag, 1985, pp. 41–67.

6. Giglio, M., Musazzi, S., and Perini, U., "Transition to Chaotic Behavior Via a Reproducible Sequence of Periodic-Doubling Bifurcations", *Physical Review Letters*, Vol. 47, No. 4, July 1981, pp. 243–246.

7. Grebogi, C., Ott, E., and Yorke, J. A., "Are Tree-Frequency Quasiperiodic Orbits to Be Expected in Typical Nonlinear Dynamical Systems?" *Physical Review Letters*, Aug. 1983, Vol. 51, No. 5, pp. 339–342.

8. Newhouse, D., Ruelle, D., and Takens, F., Occurance of Strange Axiam A Attractors Near Quasi-Periodic Flows on Tm, , *Communication in Mathematics and Physics*, Vol. 64, No. 35, 1978.

9. Dowell, E. H., "Chaotic Oscillations in Mechanical System", *Computational Mechanics*, Springer-Verlag, Vol. 3, 1988, pp. 199–216.

10. Zeng, X., Eykholt, R., and Pielke, R. A., "Estimating the Lyapunov Exponent Spectrum From Short Time Series of Low Precision", *Physical Review Letters*, Vol. 66, No. 25, June 1991, pp. 3229–3232.

11. Matsumoto, J. C., and Tsuda, I., "Noise-Induced Order". *Journal Statistical Physics*, Vol. 31, No. 87, 1983, pp. 87–106.

12. Sirovich, L., Ball, K. S., and Keefe, L. R., "Pane. Wave on Structures in Turbulent Channel Flow", *Physics Fluids*, Vol. A2, No. 12, Dec. 1990.

13. Ribner, H. S., "Boundary Layer Induced Noise in the Interior of Aircraft", University of Toronto, Institute of Aerophysics, Rept. No. 37, 1958.

14. Maestrello, L., "Design Criterion of Panel Structure Excited by Turbulent Boundary Layer", *Journal of Aircraft*, Vol. 5, No. 4, 1968, p. 321.

15. Hurre, P., and Monkewitz, P. A., "Local and Global Instabilities in Spatially Developing Flow", *Annual Review of Fluid Mechanics*, Vol. 22, 1990, pp. 473–537.

16. Michalke, A., "Survey on Jet Instability Theory", *Progress in Aerospace Science*, Vol. 21, 1984, pp. 159–199.

17. Fenno, C. C., Bayliss, A., and Maestrello, L., "Panel Structure Response to Acoustic Forcing by Nearly Sonic Jet", *AIAA Journal*, Vol. 35, No. 2, 1997, pp. 219–227.

18. Flesselles, J. M., Croquette, V., and Jucquois, S., "Periodic Doubling of a Torus in a Chain of Oscillators", *Physical Review Letters*, Vol. 72, No. 18, May 1994, pp. 2871–2874.

19. Von Stamm, J., Gerdts, U., Buzug, Th., and Pfister, G., "Symmetry Breaking and Period Doubling on a Torus in the VLF Regime in Taylor-Couette Flow", *Physical Review E*, Vol. 54, No. 5, Nov. 1996, pp. 4938–4957.

20. Chow, P. L., and Maestrello, L., "Stability of Non-Linear Panel Vibration by Boundary Layer Damping", *Journal of Sound and Vibration*, Vol. 182, No. 4, 1995, pp. 541–558.

21. Dowell, E. H., and Pezeshki, C., "On the Understanding of Chaos in Duffing Equation Including a Comparison With Experiment", *Journal of Applied Mechanics*, Vol. 53, No. 1, 1986, pp. 5–9.

22. Franceschini, V., "Bifurcations of Tori and Phase Locking in a Dissipative System of Differential Equations", *Pysica*, Vol. 6D, 1983, pp. 285–304.

23. Maestrello, L., Frendi, A., and Brown, D. E., "Nonlinear Vibration and Radiation From a Panel With Transition to Chaos", *AIAA Journal*, Vol. 30, No. 11, Nov. 1992, pp. 4938–4957.

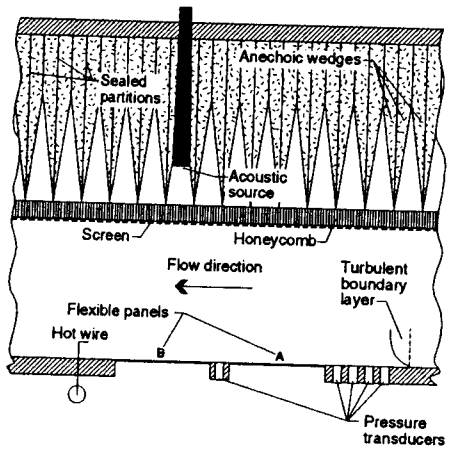

Fig. 1. Top view of wind tunnel set-up with anechoic test section.

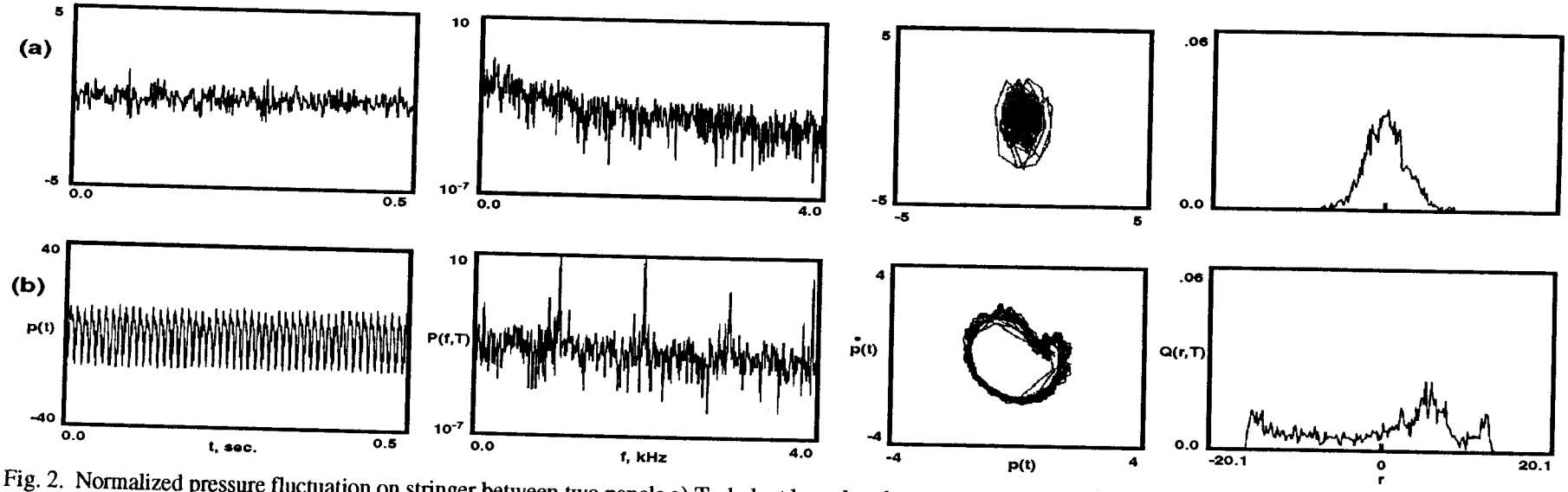

Fig. 2. Normalized pressure fluctuation on stringer between two panels a) Turbulent boundary layer without external sound and b) Turbulent boundary layer with external pure tone sound.

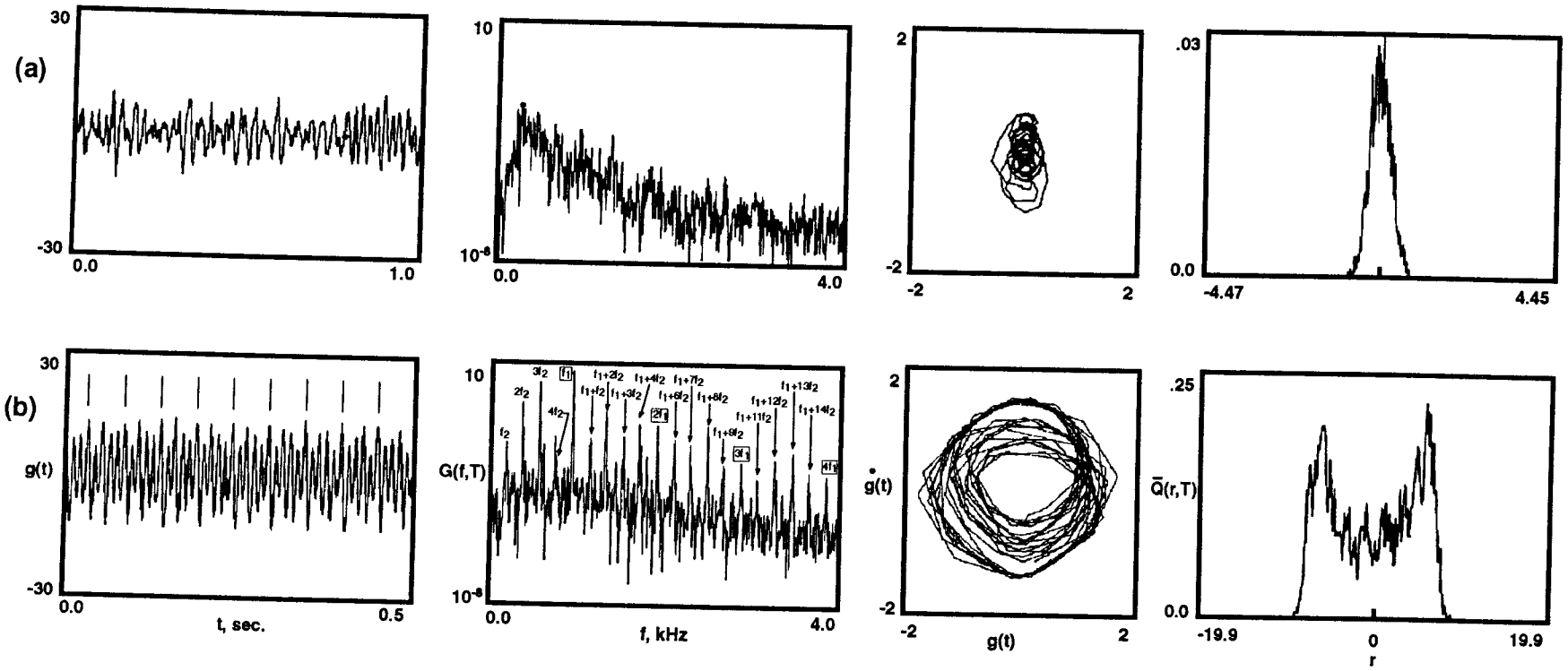

Fig. 3. Panel normalized acceleration responses a) Turbulent boundary layer without external sound b) Turbulent boundary layer with external pure tone sound.

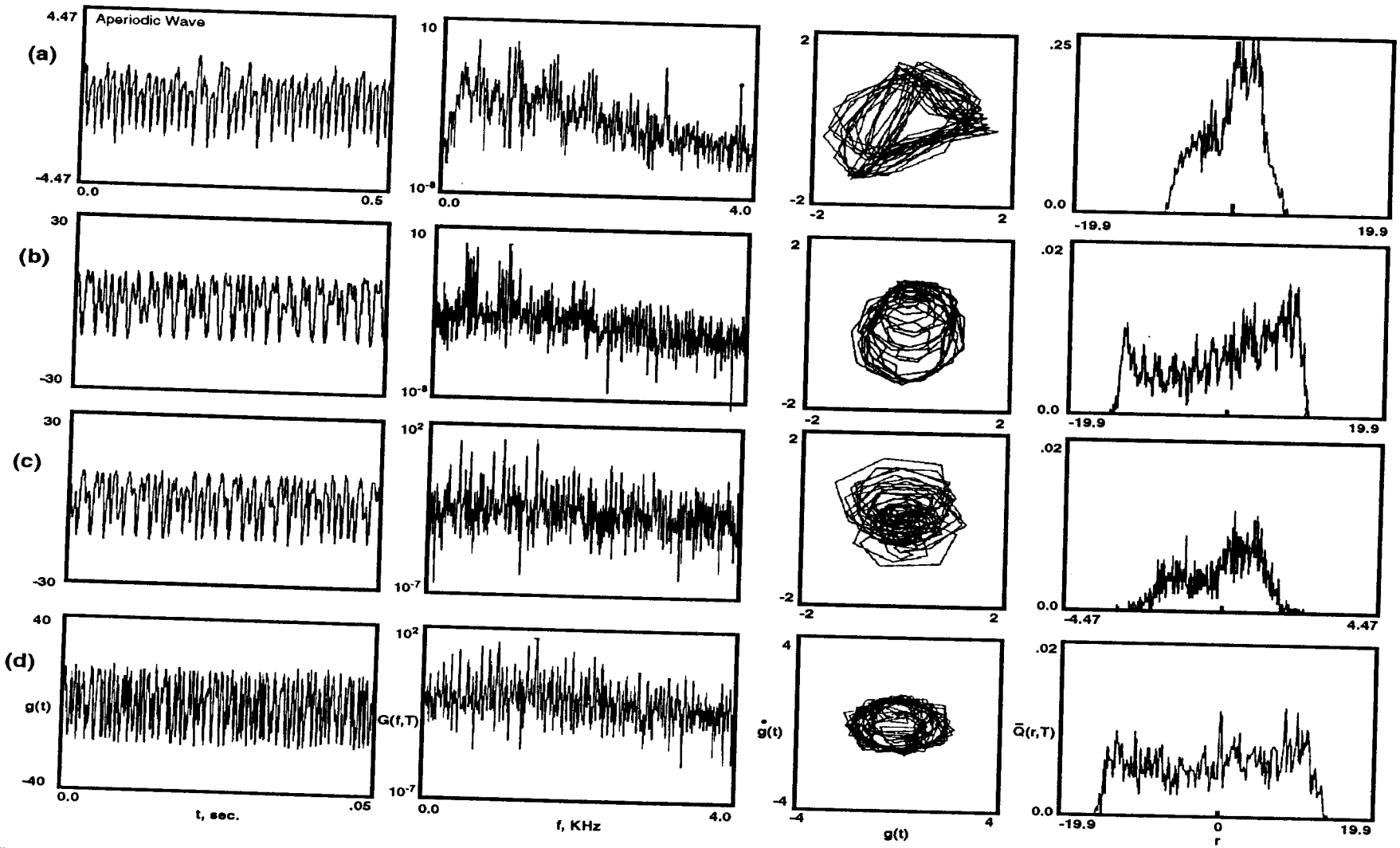

Fig. 4. Normalized panel acceleration response. with turbulent boundary layer and external pure tone sound a) low order chaos at 1/4 panel length b) low order chaos at 3/4 panel length c) broadband chaos response at 1/4 panel length and d) broadband chaos at 3/4 panel length.

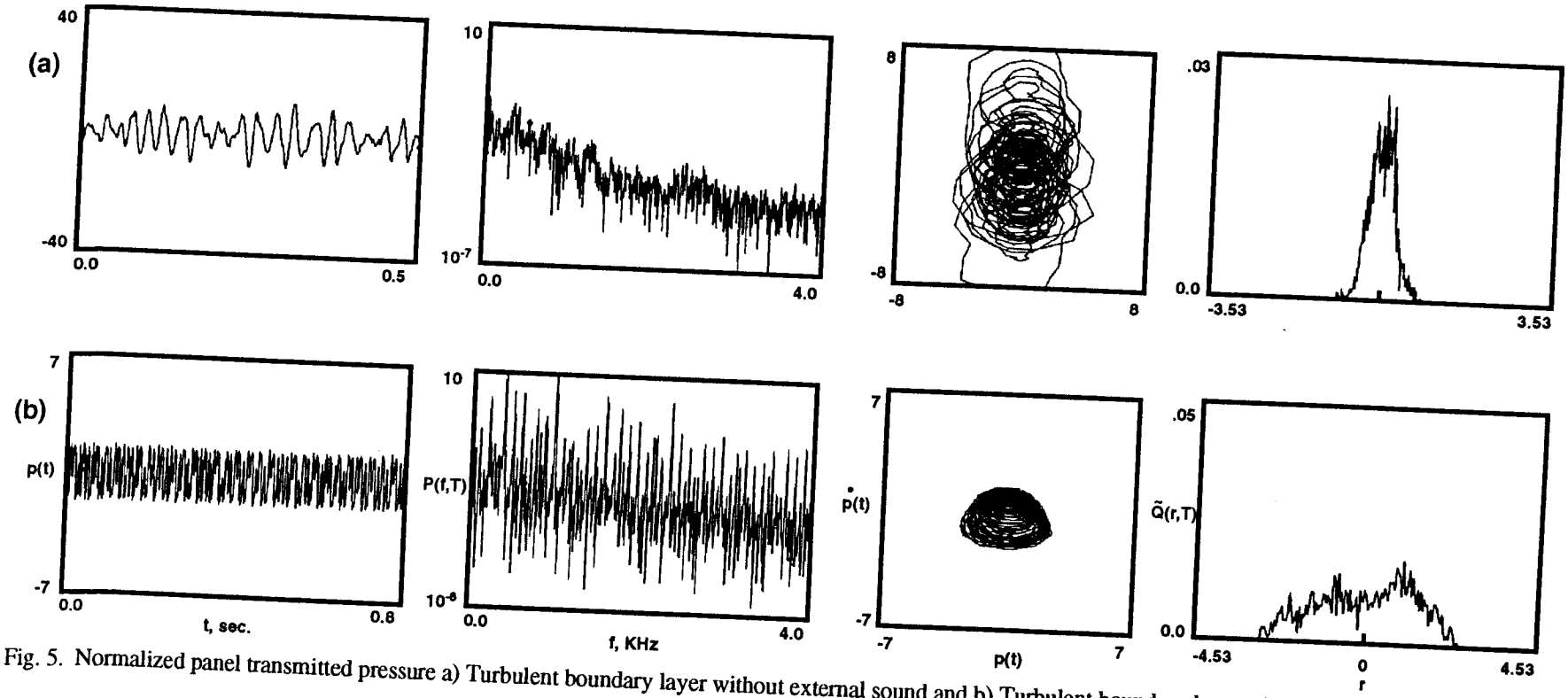

Fig. 5. Normalized panel transmitted pressure a) Turbulent boundary layer without external sound and b) Turbulent boundary layer with external pure tone sound